PHOTOMETRIC DIAGNOSTICS OF PLASMA OF PLANAR CAPACITIVE RF DISCHARGE IN ARGON AT 1 atm PRESSURE

V.Yu. Bazhenov[1], S.M. Gubarev[1], V.V. Tsiolko[1], D.S. Levko[2]
[1]Institute of Physics NAS of Ukraine, Kyiv, Ukraine;
[2]CFDR Corporation, Huntsville, USA
E-mail: gubarev@iop.kiev.ua

The results of study of the plasma parameters of radio frequency capacitive discharge with isolated electrodes in atmospheric-pressure argon by means of bremsstrahlung photometry in wavelength range 400…600 nm are presented. Time-averaged spatial distributions of the plasma electron temperature are experimentally obtained for low-current α-and high-current γ-modes of the discharge glow. The comparison of the experimental results with the preliminary data of the discharge computer modeling by a particle-in-cell method is presented.

PACS: 52.80.Pi

INTRODUCTION

Capacitive radio-frequency (RF) atmospheric-pressure discharges are widely used in different technological processes such as plasma sterilization of medical instruments [1, 2], surface treatment of various materials [3, 4], creation of layers for liquid crystal alignment [5], plasma-chemical processes etc. Such discharge is one of the most attractive ones due to low breakdown voltage, ability to create uniform plasma with high concentration of active species in relatively large volume, and low gas temperature.

One of the most important plasma parameters is the electron temperature since it defines the rates of many plasma-chemical reactions and, consequently, concentrations of active species in the plasma. Efficient non-perturbing method of determining the plasma parameters is based on optical emission spectroscopy.

In the non-thermal weakly ionized plasma of atmospheric-pressure RF discharge, main source of continuum emission in visible spectrum range is one originated from electron bremsstrahlung at neutral atom. Intensity of such plasma emission in approximation of maxwellian electron energy distribution function (EEDF) is defined by the expression:

$$\epsilon_{ea} \propto \frac{n_e n_a}{\lambda^2} \frac{1}{(kT_e)^{3/2}} \int_{hc/\lambda}^{\infty} Q_{ea}(\lambda, E)\, E\, e^{-E/kT_e}\, dE, \quad (1)$$

where n_e is the electron concentration, n_a is the concentration of working gas atoms, λ is the emission wavelength, k – is the Boltzmann constant, T_e is the electron temperature, Q_{ea} is the neutral bremsstrahlung cross section, E is the electron energy.

Photometric method of non-perturbing study of T_e spatial distribution was proposed in [6] and used in [7] for determining this distribution in atmospheric-pressure RF discharge plasma by measurement of its neutral bremsstrahlung emission. At that, the discharge cross section images were obtained by DSLR camera with spectrum selection performed by sequentially used two narrow band (1.5 nm FWHM) interference filters having transmission maxima at 514.5 and 632.8 nm, and T_e distribution across the discharge was determined from respective ratios of neutral bremsstrahlung intensities at two selected wavelengths for each point of the discharge image. In spite of the averaging data of multiple discharge images in [7], the authors did not succeed in obtaining good signal-to-noise ratio and presented only rough noisy T_e spatial distribution.

In the present paper, the method proposed in [6, 7] is essentially improved due to the bremsstrahlung emission spectrum selection performed by inherent color separation of DSLR camera sensor in broad blue and green spectrum bands (about 100 nm FWHM each). At that, no additional spectrum filtering elements are required, and single image of the discharge plasma emission is sufficient for determining T_e spatial distribution with good signal-to-noise ratio.

The present paper continues our previous studies [8] utilizing photometric methods for space-resolved characterization of plasma parameters of RF atmospheric pressure discharges. Time-averaged electron temperature distributions are determined experimentally for different regimes of the discharge glow. These results are compared with the preliminary data of the discharge numerical simulation performed by a particle-in-cell (PIC) method.

1. EXPERIMENTAL SETUP AND METHODS

Scheme of the experimental setup is shown in Fig. 1. Capacitive RF (13.56 MHz) discharge glowed between two flat electrodes covered by 1 mm thick alumina plates 5. The dimensions of each electrode were 1 x 5 cm and the gas gap between the plates was 1 mm. Industrial RF generator 7 (MV-1.5, JSC "Selmi") operating at 13.56 MHz frequency was used for powering the discharge. Voltage after matching unit 6 was varied in the range 0 to 1600 V RMS during our experiments. The discharge electrodes were powered via capacitive dividers (C1-C2, C3-C4). Volumetric consumption of the working gas argon was controlled by means of the gas feeding system and comprised 3 liters per minute.

Emission of the RF discharge plasma was registered by means of the digital reflex camera Canon-EOS-350D used at low sensitivity setting of 200 international standardization organization (ISO) units for reducing

camera sensor noise. Experimentally optimized exposure time of 1/15 s provided time-averaged detection of the discharge plasma emission. Discharge space image at the camera sensor scaled 1:1 was formed by quartz achromatic lens with 150 mm focal length and 15 mm diameter. Special attention was devoted to obtaining depth of field (DOF) distance of 1 cm required for correct (non-overlapped) observation of the plasma emission from the whole discharge thickness. Taking into account the uniform discharge glow over the whole square of the electrodes, the above condition should be fulfilled only in the direction perpendicular to the discharge plane. For that purpose, the lens aperture in this direction was reduced to 5 mm by means of slit 2. Such arrangement enabled 1 cm diffraction limited DOF, and corresponding resolution in the image plane was about 50 μm FWHM.

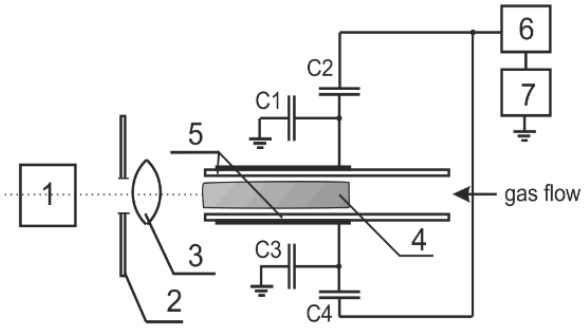

Fig. 1. A scheme of the experimental setup. 1 – DSLR camera; 2 – aperture; 3 – lens; 4 – plasma in the discharge space; 5 – dielectric barriers; 6 – impedance matching unit; 7 – RF generator (13.56 MHz)

The camera sensor pixels responsible for red, green and blue color channels are known to be arranged by means of the Bayer color filter array so that each elementary cell of the array consists of one blue, two green and one red pixels. For enabling photometric studies, the sensor readout should be done without any post-processing. In our experiments, it was performed by UFRaw software which linearly converted camera RAW files to 16 bit per color channel TIFF images used for subsequent consideration. In our experiments, only blue and green color channels embracing about 400…600 nm spectrum range were used for bremsstrahlung emission measurements because red channel was affected by the presence of atomic argon emission lines.

For precise photometric spectrum-integrated measurements for particular color channel, one should exactly know the spectrum sensitivity of each channel. This calibration procedure was performed by MDR-23 monochromator combined with the standard spectroscopic tungsten incandescent lamp (2850 K color temperature). This system provided spectrum selection with about 1 nm bandwidth tunable with 10 nm steps over the spectrum range of interest. At each step, the RAW image was taken and subsequently converted by mentioned above procedure with UFRaw software use. At that, all settings of the conversion were the same as ones used later for bremsstrahlung emission study. The spectrum sensitivity curves for particular camera obtained by the calibration procedure are shown in Fig. 2. Almost two times lower sensitivity of green channel is due to the fact that digital readout of the sensor in green channel is done from twice bigger number of green pixels in Bayer array of the camera sensor.

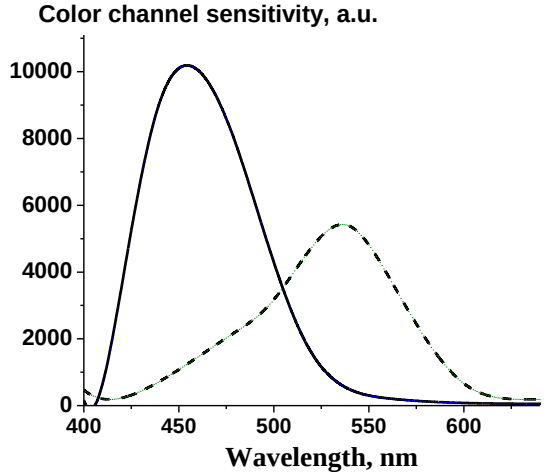

Fig. 2. Color channel spectral sensitivity of DSLR camera Canon-EOS-350D. Solid line – for blue channel, dash line – for green channel

As it was already noted, the discharge glows uniformly over the whole square of the electrodes, so that it could be characterized only by the spatial profile measurements of blue to green readout ratio across the electrode plane. Mentioned profile was obtained by means of ImageJ software which performed data averaging for about 3000 image pixels along the electrode plane. This allowed us to obtain good signal-to-noise ratio from the data of single discharge image thus making the described approach attractive for express consideration of the discharge plasma features.

For determining T_e spatial distribution, one should define the relation between the data of photometric experiment and the electron temperature. Such procedure has been done earlier in [6, 7] for the case of the bremsstrahlung intensity measurements at two spectrum points. We modified mentioned procedure for the case of spectrum-integrated intensity measurements. For that purpose, the ratios of blue to green values of convolution between the bremsstrahlung plasma emission spectrum calculated using (1) and wavelength dependence of the camera sensor sensitivity for respective color channel on wavelength $q(\lambda)$ were calculated for different T_e. It should be noted that the calculated ratio $(\varepsilon_{ea}(\lambda)\cdot q_{blue}(\lambda)) / (\varepsilon_{ea}(\lambda)\cdot q_{green}(\lambda))$ is a function of the electron temperature T_e and does not depend on the electron concentration. Calculated in such a way dependence for particular Canon EOS-350D digital camera used in our experiments is presented in Fig. 3. One can easily see from the dependence shape that it can be used for unambiguous solving the inverse problem, that is determining T_e spatial distribution by measured blue-to-green readout ratios from the discharge image.

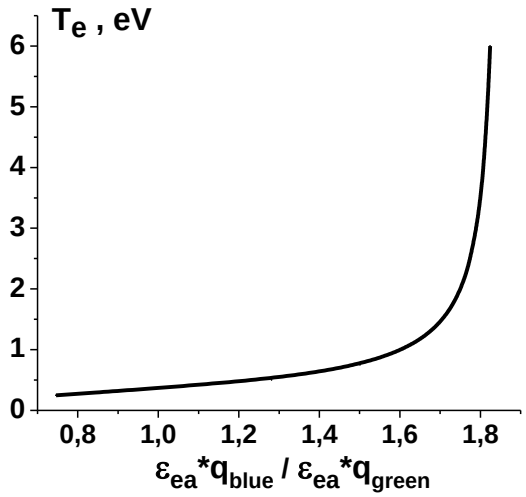

Fig. 3. Calculated relation between RF discharge plasma electron temperature T_e and blue-to-green readout ratio of Canon EOS-350D camera sensor

2. EXPERIMENTAL DATA AND DISCUSSION

The described above procedure allowed us to obtain the time-averaged spatial distribution of the electron temperature T_e^{exp} across the discharge gap as the function of the discharge current density j (Fig. 4). It should be noted that no additional averaging of the experimental data was done along the direction denoted as L in (see Fig. 4), and all existing irregularities were exactly reproducible for repeatedly taken discharge images for each discharge glow mode.

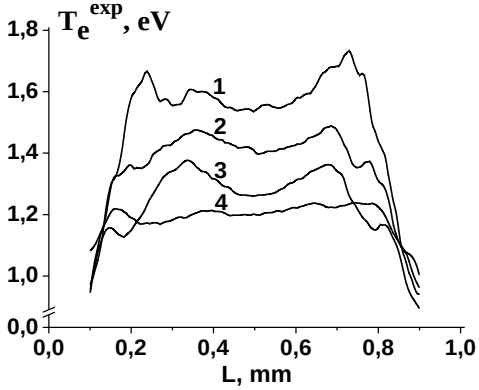

Fig. 4. Time-averaged spatial distribution of experimentally determined electron temperature T_e^{exp} for different discharge glow modes: 1 – j = 37 mA/cm^2; 2 – j = 54 mA/cm^2; 3 – j = 75 mA/cm^2; 4 – j = 147 mA/cm^2

One can see that the transition from the low-current α – (j = 37 mA/cm^2) to the high-current γ-mode (j = 147 mA/cm^2) the electron temperature T_e^{exp} in the bulk plasma gradually decreases from ≈ 1.6 to ≈ 1.2 eV. The large-scale irregularities, that is, the asymmetry with respect to the central plane of the discharge gap (L = 0.5 mm), are most probably due to the technical issues such as the influence of the electrically grounded laboratory environment on horizontally placed discharge unit. The small-scale irregularities are definitely due to the discharge nature and could actually have higher amplitude due to the imaging system diffraction-limited optical resolution of about 50 μm. This fact could be also responsible for the absence of T_e^{exp} maxima near the electrodes (L ≤ 0.1 mm and L ≥ 0.9 mm) which might be expectable in high-current discharge glow modes.

Here it is worth to clarify some peculiarities of the method. Actually, electrons with the energies corresponding to the experimentally determined T_e^{exp} (E < 2 eV) do not contribute to the studied bremsstrahlung emission because their energy is insufficient for light radiation in the visible spectrum range. On another side, high energy electrons (E >> 2 eV) also do not make essential contribution to the plasma emission due to the rapid decrease of their concentration $\sim e^{-E / kTe}$. Thus, obtained data make direct characterization the discharge plasma only in the limited range of the electron energy. Experimentally obtained T_e^{exp} is essentially based on the assumption of the Maxwellian EEDF. It is commonly accepted that the actual EEDF in the intermediate α-γ and high-current γ-mode of RF discharge can deviate from the Maxwellian one. Actual influence of this circumstance on the accuracy of the obtained results is a subject of future investigations.

As the initial step of the validation of the obtained experimental data, preliminary numerical simulation of the RF discharge was carried out by PIC code [9] for the simulation parameters close to the experimental data. The spatial distribution of the time-averaged effective electron temperature T_e^{calc} in the discharge gap is shown in Fig. 5. This T_e^{calc} was defined as 2/3 of the mean electron energy determined from the simulated EEDF.

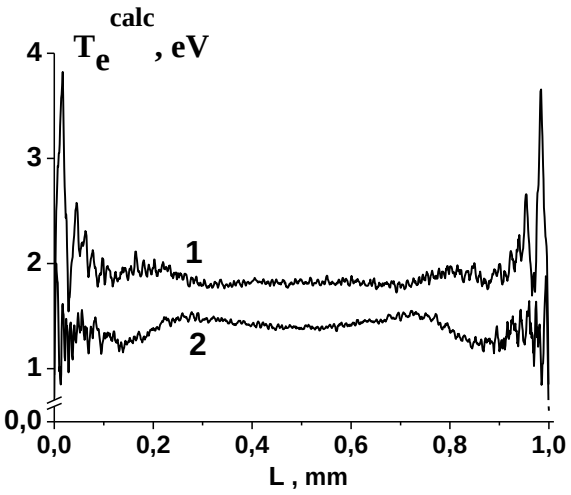

Fig. 5. Time-averaged spatial distribution of electron temperature T_e^{calc} calculated by numerical simulation of RF discharge plasma: 1 – α-γ-mode; 2 – γ-mode

It was found that simulated electron temperature T_e^{calc} in the plasma bulk decreases for increasing discharge current which is in qualitative agreement with

the results of our experimental studies. The modeling has shown essential EEDF modulation during RF oscillation cycle due to the fast relaxation of the electron energy.

CONCLUSIONS

The advanced photometric method to determine the plasma electron temperature in the atmospheric-pressure RF discharge was proposed and tested. In this method, the digital camera imaging of the electron – neutral atom bremsstrahlung emission from the discharge space in 400…600 nm spectrum range is recorded and analyzed. The experimentally determined time-averaged spatial distributions of the plasma electron temperature in the planar capacitive RF discharge in the atmospheric-pressure argon demonstrate gradual temperature decrease from ≈ 1.6 to 1.2 eV at the discharge glow mode transition from low-current α-($j = 37$ mA/cm^2) to high-current γ-mode ($j = 147$ mA/cm^2). Spatial distributions of the plasma electron temperature derived from numerical modeling by means of PIC method are in qualitative agreement with obtained experimental data.

Proposed photometric method of determining plasma electron temperature value and spatial distribution can be used as express technique for diagnostics of weakly ionized plasma of atmospheric pressure RF discharges and their optimization for different practical applications.

REFERENCES

1. T. Akitsu, H. Ohkawa, M. Tsuji, H. Kimura, M. Kogoma. Plasma sterilization using glow discharge at atmospheric pressure // *Surface and Coatings Technology*. 2005, v. 193, № 1, p. 29-34.
2. F. Iza, G.J. Kim, S.M. Lee, J.K. Lee, J.L. Walsh, Y.T. Zhang, M.G. Kong. Microplasmas: Sources, Particle Kinetics, and Biomedical Applications // *Plasma Processes and Polymer*. 2008, v. 5, № 4, p. 322-344.
3. M. Moravej, R.F. Hicks. Atmospheric Plasma Deposition of Coatings Using a Capacitive Discharge Source // *Chemical Vapor Deposition*. 2005, v. 11, p. 469-476.
4. J.Y. Jeong, S.E. Babayan, V.J. Tu, J. Park, I. Henins, R.F. Hicks, G.S. Selwyn. Etching materials with an atmospheric-pressure plasma jet // *Plasma Sources Science and Technology*. 1998, v. 7, p. 282-285.
5. V.Yu. Bazhenov, R.Yu. Chaplinskiy, R.M. Kravchuk, A. Kuzmichev, V. Piun, V. Tsiolko, O. Yaroshchuk. Treatment of polyimide films by an atmospheric pressure plasma of capacitive RF discharge for liquid crystal alignment // *Problems of Atomic Science and Technology. Series "Plasma Physics"*. 2013, v. 83, p. 177-179.
6. S. Park, W. Choe, H. Kim, J.Y. Park. Continuum emission-based electron diagnostics for atmospheric pressure plasmas and characteristics of nanosecond-pulsed argon plasma jets // *Plasma Sources Science and Technology*. 2015, v. 24, № 3, p. 034003.
7. S. Park, W. Choe, S.Y. Moon, S.J. Yoo. Spatio-temporally resolved electron temperature in argon radio-frequency capacitive discharge at atmospheric pressure // *Plasma Sources Science and Technology*. 2015, v. 24, № 3, p. 032006.
8. V.Yu. Bazhenov, S.M. Gubarev, V.V. Tsiolko, R.Yu. Chaplinskiy. Spatial distribution of continuum radiation from plasma of planar capacitive RF discharge in argon at 1 atm pressure: photometric study // *Problems of Atomic Science and Technology. Series "Plasma Physics"*. 2016, v. 80, p. 199-202.
9. D. Levko, L.L. Raja. Breakdown of atmospheric pressure microgaps at high excitation frequencies // *Journal of Applied Physics*. 2015, v. 117, p. 173303.

Article received 28.09.2018

ФОТОМЕТРИЧЕСКАЯ ДИАГНОСТИКА ПЛАЗМЫ ПЛАНАРНОГО ЕМКОСТНОГО ВЧ-РАЗРЯДА В АРГОНЕ ПРИ ДАВЛЕНИИ 1 атм

В.Ю. Баженов, С.Н. Губарев, В.В. Циолко, Д.С. Левко

Представлены результаты исследования параметров плазмы высокочастотного емкостного разряда с изолированными электродами в аргоне атмосферного давления методом фотометрии ее тормозного излучения в спектральном диапазоне ≈ 400…600 нм. Экспериментально получены усредненные по времени пространственные распределения температуры электронов плазмы в слаботочном α- и сильноточном γ-режимах горения разряда. Представлено сравнение экспериментальных результатов с предварительными данными компьютерного моделирования разряда методом частиц в ячейке.

ФОТОМЕТРИЧНА ДІАГНОСТИКА ПЛАЗМИ ПЛАНАРНОГО ЄМНІСНОГО ВЧ-РОЗРЯДУ В АРГОНІ ПРИ ТИСКУ 1 атм

В.Ю. Баженов, С.М. Губарєв, В.В. Ціолко, Д.С. Левко

Наведено результати дослідження параметрів плазми високочастотного ємнісного розряду з ізольованими електродами в аргоні атмосферного тиску методом фотометрії її гальмівного випромінювання в спектральному діапазоні ≈ 400…600 нм. Експериментально отримано усереднені за часом просторові розподіли температури електронів плазми в слабкострумовому α- та сильнострумовому γ-режимах горіння розряду. Представлено порівняння експериментальних результатів з попередніми даними комп'ютерного моделювання розряду методом часток у комірці.